Oncogene (2009), 1–13

www.nature.com/onc

ORIGINAL ARTICLE

Matrix Metalloproteinase-9 gene induction by a truncated oncogenic NF-κB2 protein involves the recruitment of MLL1 and MLL2 H3K4 histone methyltransferase complexes

I Robert[1,2,3], M Aussems[1,2,3], A Keutgens[1,2,3], X Zhang[1,2,3], B Hennuy[1,4], P Viatour[1,2,3], G Vanstraelen[1,5], M-P Merville[1,2,3], J-P Chapelle[1,2,3], L de Leval[1,6], F Lambert[1,7], E Dejardin[1,2,8], A Gothot[1,5] and A Chariot[1,2,3]

[1]*Interdisciplinary Cluster for Applied Genoproteomics (GIGA-R), CHU, Sart-Tilman, University of Liege, Liege, Belgium;* [2]*GIGA Signal Transduction, CHU, Sart-Tilman, University of Liege, Liege, Belgium;* [3]*Laboratory of Medical Chemistry, CHU, Sart-Tilman, University of Liege, Liege, Belgium;* [4]*GIGA Transcriptomics Facility, CHU, Sart-Tilman, University of Liege, Liege, Belgium;* [5]*Department of Medicine/Hematology, CHU, Sart-Tilman, University of Liege, Liege, Belgium;* [6]*Department of Pathology, CHU, Sart-Tilman, University of Liege, Liege, Belgium;* [7]*Laboratory of Human Genetics, CHU, Sart-Tilman, University of Liege, Liege, Belgium and* [8]*Laboratory of Virology and Immunology, CHU, Sart-Tilman, University of Liege, Liege, Belgium*

Constitutive nuclear factor (NF)-κB activation in haematological malignancies is caused in several cases by loss of function mutations within the coding sequence of NF-κB inhibitory molecules such as IκBα or p100. Hut-78, a truncated form of p100, constitutively generates p52 and contributes to the development of T-cell lymphomas but the molecular mechanism underlying this oncogenic potential remains unclear. We show here that *MMP9* gene expression is induced through the alternative NF-κB-activating pathway in fibroblasts and also on Hut-78 or p52 overexpression in fibroblasts as well as in lymphoma cells. p52 is critical for Hut-78-mediated *MMP9* gene induction as a Hut-78 mutant as well as other truncated NF-κB2 proteins that are not processed into p52 failed to induce the expression of this metalloproteinase. Conversely, *MMP9* gene expression is impaired in p52-depleted HUT-78 cells. Interestingly, MLL1 and MLL2 H3K4 methyltransferase complexes are tethered by p52 on the *MMP9* but not on the *IκBα* promoter, and the H3K4 trimethyltransferase activity recruited on the *MMP9* promoter is impaired in p52-depleted HUT-78 cells. Moreover, MLL1 and MLL2 are associated with Hut-78 in a native chromatin-enriched extract. Thus, we identified a molecular mechanism by which the recruitment of a H3K4 histone methyltransferase complex on the promoter of a NF-κB-dependent gene induces its expression and potentially the invasive potential of lymphoma cells harbouring constitutive activity of the alternative NF-κB-activating pathway.
Oncogene advance online publication, 16 February 2009; doi:10.1038/onc.2009.6

Keywords: NF-κB; MMP9; H3K4 HMT; p100

Correspondence: Dr A Chariot, Laboratory of Medical Chemistry, Interdisciplinary Cluster for Applied Genoproteomics, Unit of Signal Transduction, GIGA-R, Tour GIGA, +2 B34, C.H.U. Sart-Tilman, University of Liege, Liege 4000, Belgium.
E-mail: Alain.chariot@ulg.ac.be
Received 14 August 2008; revised 15 December 2008; accepted 19 December 2008

Introduction

Most haematological disorders remarkably share a constitutive nuclear factor (NF)-κB activity (Karin and Lin, 2002; Courtois and Gilmore, 2006; Keutgens *et al*., 2006; Jost and Ruland, 2007; Perkins, 2007). NF-κB is a latent cytoplasmic transcription factor whose activation is regulated via control of nuclear translocation through the signal-induced degradation of inhibitory proteins (Hayden and Ghosh, 2008). Two main NF-κB-activating signalling pathways have been characterized and referred to as the 'classical' or 'canonical' pathway and the 'alternative' or 'non-canonical' pathway (Bonizzi and Karin, 2004). The classical pathway, which is triggered by cytokines such as tumor necrosis factor-α (TNFα), interleukin (IL)-1β, or by the ligand for the T-cell or B-cell receptor, leads to IκBα degradation and subsequent nuclear import of the p50/p65 heterodimer through a NEMO/IKKγ-dependent pathway (Li and Verma, 2002; Shim *et al*., 2005). The alternative pathway, which is triggered by cytokines such as lymphotoxin-β (LTβ), BAFF and CD40, relies on the NIK- and IKKα-mediated phosphorylation and processing of the inhibitory protein p100 into p52. As a result, a p52/RelB heterodimer moves into the nucleus and induces the expression of proteins involved in lymphoid organogenesis and B-cell homeostasis (Claudio *et al*., 2002; Coope *et al*., 2002; Dejardin *et al*., 2002).

NF-κB acts as a survival factor from early lymphopoiesis to later stage of development and maturation of B and T cells (Siebenlist *et al*., 2005). The constitutive NF-κB activity seen in most haematological disorders occurs through several mechanisms, including the chromosomal translocation and subsequent overexpression of BCL-3 in a subset of human B-cell chronic lymphotic leukaemias (McKeithan *et al*., 1987) and mutations of the *IκBα* gene that impair its inhibitory function in some cases of Hodgkin's lymphomas (Cabannes *et al*., 1999; Emmerich *et al*., 1999; Jungnickel *et al*., 2000). Gene amplification of *NIK* or loss of

function mutations for inhibitory signalling molecules such as TRAF3 and CYLD have been reported in multiple myelomas (Annunziata *et al*., 2007; Keats *et al*., 2007).

Rearrangement of the *nf-κb2* gene has been described in some cutaneous T-cell lymphomas, B-cell chronic lymphocytic leukemias (CLLs), multiple myelomas and B-cell lymphomas (Keutgens *et al*., 2006). These translocations cause the expression of truncated p100 proteins referred to as Lyt-10-Cα, LB40 or Hut-78/p85/p80HT, that differ in their C-terminal end (Neri *et al*., 1991; Fracchiolla *et al*., 1993; Thakur *et al*., 1994). Those proteins are nuclear and constitutively generate p52 because of the loss of the C-terminal processing-inhibitory domain of p100 (Zhang *et al*., 1994; Chang *et al*., 1995; Xiao *et al*., 2001). Mice with a homozygous deletion of the C-terminal ankyrin repeats of p100, which allows them to express p52 but not the inhibitory protein p100, suffered from gastric hyperplasia and also showed enlarged lymph nodes and increased proliferation of peripheral lymphocytes (Ishikawa *et al*., 1997). Interestingly, a transgenic mouse overexpressing a lymphoma-associated NF-κB2 mutant Hut-78 in lymphocytes developed small B-cell lymphomas, in part through the upregulation of the antiapoptotic protein TRAF1 (Zhang *et al*., 2007).

The progression of T-cell lymphoma towards a metastatic phenotype is associated with the upregulation of MMP9, which plays key roles in degradation of extracellular matrix and in vascular remodelling (Lalancette *et al*., 2000; Heissig *et al*., 2003). MMP9 is also critical for B-CLL invasion and progression and has been defined as a prognostic factor in patients with non-Hodgkin's lymphoma (Sakata *et al*., 2004; Redondo-Munoz *et al*., 2006). The transcriptional induction of MMP9 is regulated by NF-κB in HTLV-I- or in Epstein–Barr virus-infected cells (Yoshizaki *et al*., 1998; Mori *et al*., 2002) as well as on TNFα stimulation in skeletal muscle cells (Srivastava *et al*., 2007). Although the classical, TAK1- and IKKβ-dependent NF-κB-activating pathway is required for the TNFα-mediated *MMP9* gene expression (Srivastava *et al*., 2007), it is unclear whether the alternative NF-κB-activating pathway is also involved in induction of MMP9 in lymphoma cells.

Here we demonstrate that the constitutively activated alternative NF-κB signalling pathway contribute to the invasive potential of lymphoma cells through induction of *MMP9* gene expression by tethering selected H3K4 methyltransferases in a promoter-specific manner.

Results

Induction of MMP9 expression on p52 or Hut-78 overexpression in transformed fibroblasts and in lymphoma cells

To gain insight into the mechanisms underlying the oncogenic potential of the truncated NF-κB2 precursors, we overexpressed p52 or Hut-78 in NIH3T3 cells through retroviral infections (Figure 1a), performed microarray analysis and noticed that *MMP9* was the most strongly induced candidate (Figure 1b). IκBα gene expression remained unchanged (data not shown) and this candidate will be used as control for the subsequent experiments. These data were confirmed by Real-time PCR analysis. Indeed, *MMP9* but not *IκBα* gene expression was induced on p52 or Hut-78 overexpression in NIH3T3 cells (Figure 1c). Although IκBα expression on p52 or Hut-78 overexpression remained unchanged, it was dramatically induced on TNFα stimulation in control NIH3T3 cells (Figure 1d). MMP9 activity was also induced as the gelatinase activities of both p52 and Hut-78 overexpressing NIH3T3 cells were enhanced compared to the ones from control or NIH3T3 cells overexpressing p100HB, another truncated p100 protein (Derudder *et al*., 2003) which barely processes into p52 (Figure 1e, top panel, compare lanes 2 and 3 with lanes 1 and 4, respectively). Thus, *MMP9* is a target gene of Hut-78 and p52 in immortalized fibroblasts. We next compared the ability of two other truncated p100 proteins, LB40 and p100HB, to induce the expression of this target gene. Although MMP9 was also strongly induced in NIH3T3 cells overexpressing the p52-producing LB40 oncogenic protein, p100HB did not induce MMP9 in those cells (Figures 2a and b). We next generated a Hut-78 mutant that failed to generate p52 because of the deletion of the glycine-rich region (GRR) domain ('Hut-78ΔGRR'; Figure 2c, bottom panel, lane 5) and tested its ability to drive MMP9 expression in NIH3T3 cells. This target gene was weakly induced in those cells (Figure 2d), indicating that *MMP9* transcriptional induction occurs through p52 overproduction. Importantly, the GRR domain of p52 was required for *MMP9* gene induction as a p52 mutant lacking this region ('p52 ΔGRR'; Figure 2c, bottom panel, lane 3) failed to induce this target gene (Figure 2d). Thus, *MMP9* gene induction by the truncated p100 proteins requires both their processing into p52 and the GRR domain.

To determine whether Hut-78-mediated *MMP9* gene induction also applies to lymphoma cells, we overexpressed Hut-78 in the lymphoma-derived cell line 164T2. RelB and p50 levels remained similar to the ones detected in control cells and only Hut-78 and p52 were overexpressed (Figure 3a, top panel, compare lanes 1 and 2). There again, Hut-78 overexpression induced MMP9 but not IκBα at the mRNA level (Figure 3b). We next depleted p100/p52 through RNA interference in HUT-78 cells and addressed MMP9 mRNA levels in those lymphoma cells (Figure 3c, second panel from the top, compare lanes 1 and 3 with lanes 2 and 4). MMP9 mRNA levels were decreased in those p52-depleted HUT-78 cells (Figure 3d). We also looked at IκBα protein levels and noticed that this product accumulated in those p52-depleted cells, which indicates that p52 may be required to repress the expression of IκBα in HUT-78 cells (Figure 3c, top panel). p52 depletion in HUT-78 cells also impaired their gelatinase activities, as evidenced by zymogram experiments (Figure 3e on the left, compare lanes 1, 3 and 5 with lanes 2, 4 and 6,

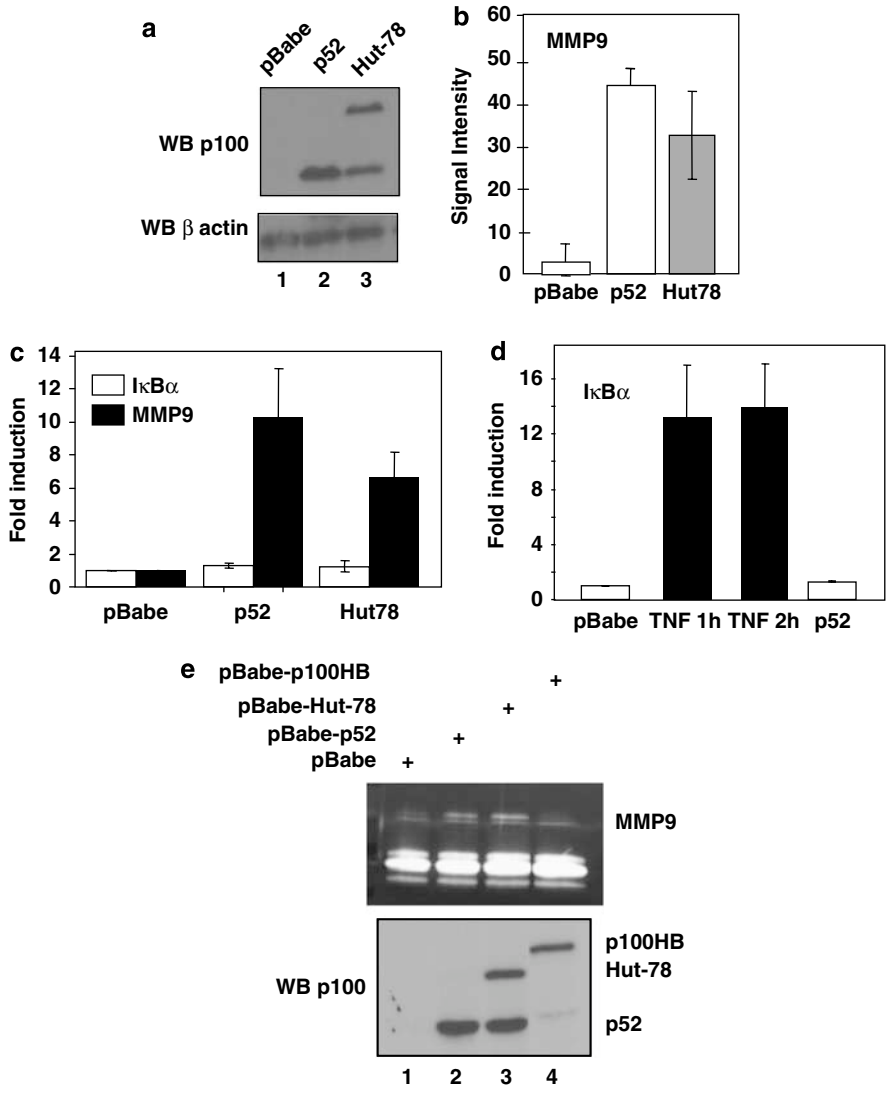

Figure 1 Induction of *MMP9* gene expression by p52 and Hut-78 in NIH3T3 cells. (**a**) Establishment of p52 or Hut-78 overexpressing NIH3T3 cells through retroviral infections. NIH3T3 cells were infected with either an empty retroviral vector (pBabe, negative control) or a retroviral construct expressing p52 or Hut-78, and cell extracts from those cells were subjected to anti-p100 or anti-β-actin western blot analysis. (**b**) Induction of *MMP9* gene expression on p52 or Hut-78 overexpression in NIH3T3 cells. Total RNAs extracted from NIH3T3 cells infected with pBabe or with a p52 or Hut-78 expressing retrovirus were subjected to microarray analysis. The figure shows microarray signal intensities from three distinct infections. Error bars denote standard deviation. (**c**) Induction of *MMP9* but not of *IκBα* gene expression on p52 or Hut-78 overexpression in NIH3T3 cells. Total RNAs from NIH3T3 cells infected with empty pBabe, the p52 or Hut-78 expressing viruses were subjected to quantitative real-time PCR analysis to assess IκBα or MMP9 mRNA levels using the appropriate primers. The abundance of the IκBα or MMP9 mRNA levels in NIH3T3 cells infected with the empty virus was set to 1 and levels of both transcripts in p52 or Hut-78 overexpressing NIHT3 cells were relative to that after normalization with glyceraldehyde-3-phosphate dehydrogenase (GAPDH). The figure shows the data from six independent experiments performed on two distinct infections (mean values ± s.d.). (**d**) Induction of *IκBα* expression on tumor necrosis factor-α (TNFα) stimulation but not on p52 overexpression in NIH3T3 cells. NIH3T3 infected with pBabe or with the p52 expressing retrovirus were left untreated or stimulated with TNFα for the indicated periods of time and the abundance of the IκBα mRNA levels was assessed by Real-Time PCR analysis. IκBα mRNA levels in untreated NIH3T3 cells infected with pBabe were set to 1 and levels of this transcript in the other experimental conditions were relative to that after normalization with GAPDH. The figure shows the data from two independent experiments performed in duplicates (mean values ± s.d.). (**e**) p52 or Hut-78 overexpression in NIH3T3 cells enhances their gelatinase activities. NIH3T3 cells were infected with the indicated retrovirus and zymograms were carried out using the supernatant from the infected cells (upper panel). An anti-p100 western blot was performed using cell extracts from these infected NIH3T3 cells (bottom panel).

respectively). Importantly, MMP9 but not MMP2 protease activity was impaired on p52 depletion in HUT-78 cells (Figure 3e, on the left, top and bottom panels), which is in agreement with our microarray results. The invasive potential of the p52-depleted HUT-78 cells was also impaired, as evidenced by Matrigel invasion assays (Figure 3e on the right). Thus, our results demonstrate that *MMP9* is a p52- and Hut-78-dependent target gene in both transformed fibroblasts and in lymphoma-derived cells and define

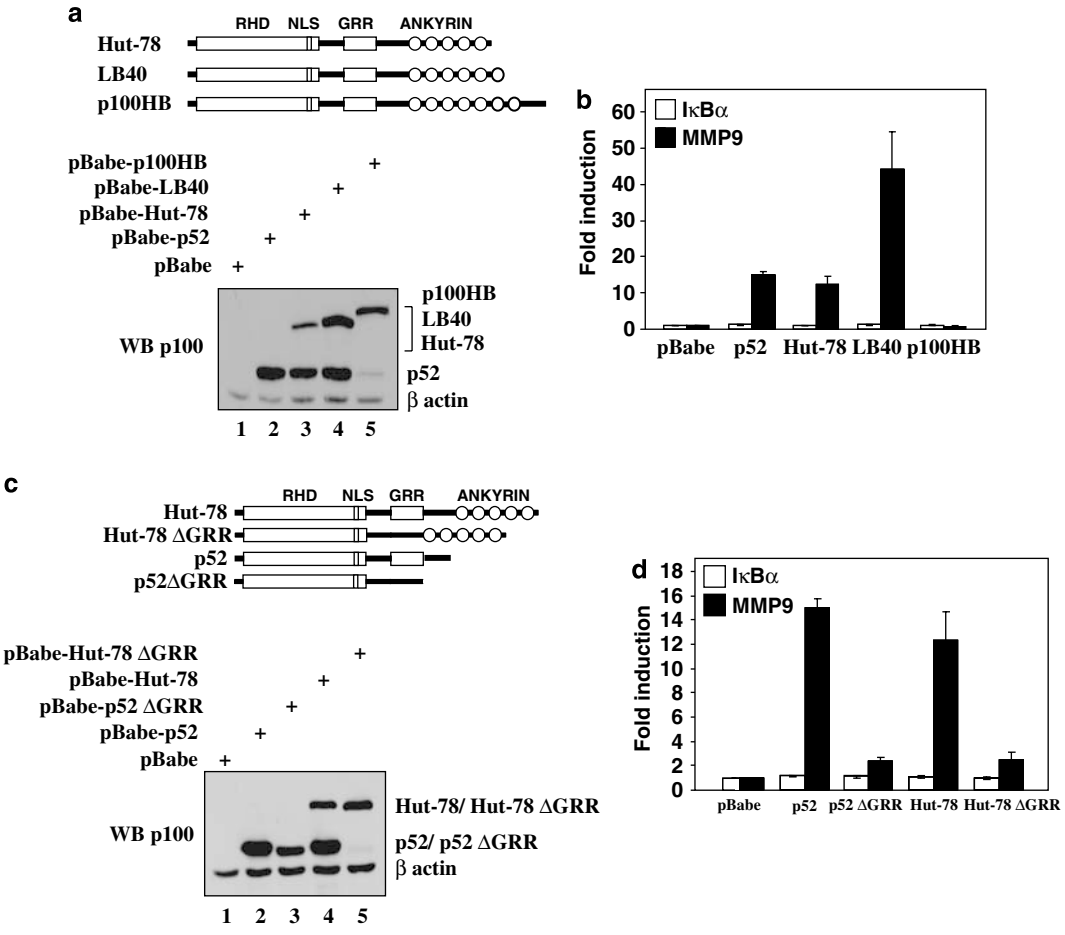

Figure 2 *MMP9* gene expression requires both constitutive p52 processing of the truncated oncogenic nuclear factor (NF)-κB2 proteins as well as the glycine-rich region (GRR) domain of p52. (**a** and **b**) *MMP9* gene induction by the p52-producing and truncated NF-κB2 proteins. (**a**) On the top, schematic representation of three distinct truncated NF-κB2 proteins (Hut-78, LB40 and p100HB). At the bottom, cell extracts from NIH3T3 cells infected with the indicated retrovirus were subjected to anti-p100 and anti-β-actin western blots. (**b**) Overexpression of both Hut-78 and LB40 but not p100HB triggers *MMP9* gene expression. Total RNAs from NIH3T3 cells infected with the indicated retrovirus were subjected to Real-Time PCR to assess MMP9 and IκBα expressions. MMP9 and IκBα mRNA levels in NIH3T3 cells infected with pBabe were set to 1 and levels of these transcripts in the other experimental conditions were relative to that after normalization with glyceraldehyde-3-phosphate dehydrogenase (GAPDH). The figure shows the data from three independent experiments performed in duplicates (mean values ± s.d.). (**c** and **d**) *MMP9* induction in NIH3T3 cells requires p52 overproduction and the GRR domain of p52. C. On the top, schematic representation of both Hut-78 and p52 proteins and a Hut-78 mutant that failed to generate p52 because of the deletion of GRR domain ('Hut-78 ΔGRR'). The p52 ΔGRR mutant is represented as well. At the bottom, cell extracts from NIH3T3 cells infected with the indicated retrovirus constructs were subjected to anti-p100 and anti-β-actin western blot analysis. (**d**) Overexpression of the Hut-78 ΔGRR mutant does not trigger *MMP9* gene expression. Total RNAs from NIH3T3 cells infected with pBabe, p52, Hut-78 or with the Hut-78 ΔGRR or the p52 ΔGRR constructs were subjected to real-time PCR to assess MMP9 and IκBα expressions. MMP9 and IκBα mRNA levels in NIH3T3 cells infected with pBabe were set to 1 and levels of these transcripts in the other experimental conditions were relative to that after normalization with GAPDH. The figure shows the data from three independent experiments performed in duplicates (mean values ± s.d.).

p52 as a key molecule for the invasive potential of lymphoma-derived cells harbouring enhanced NF-κB activity.

MMP9 induction via both the classical and the alternative NF-κB-activating pathways

To explore whether the alternative NF-κB-activating pathway, which mainly relies on the p52/RelB heterodimer, drives MMP9 expression, we first stimulated mouse embryonic fibroblast (MEF) cells with a LTβR agonistic antibody, which is known to trigger both the classical and the alternative NF-κB-activating pathways (Dejardin *et al*., 2002). As control, we stimulated those cells with TNFα. As expected, the LTβR agonistic antibody, but not TNFα, induced p100 processing into p52 (Figure 4a, top panel, compare lane 2–4 with lane 1 and lanes 5–7 with lane 1). Both *IκBα* and *MMP9* gene expression were induced on TNFα or LTβ stimulation, although the kinetic of these inductions was different (Figures 4c and d, respectively). We repeated those experiments in NEMO-deficient cells in which the classical NF-κB-activating pathway is abolished. As

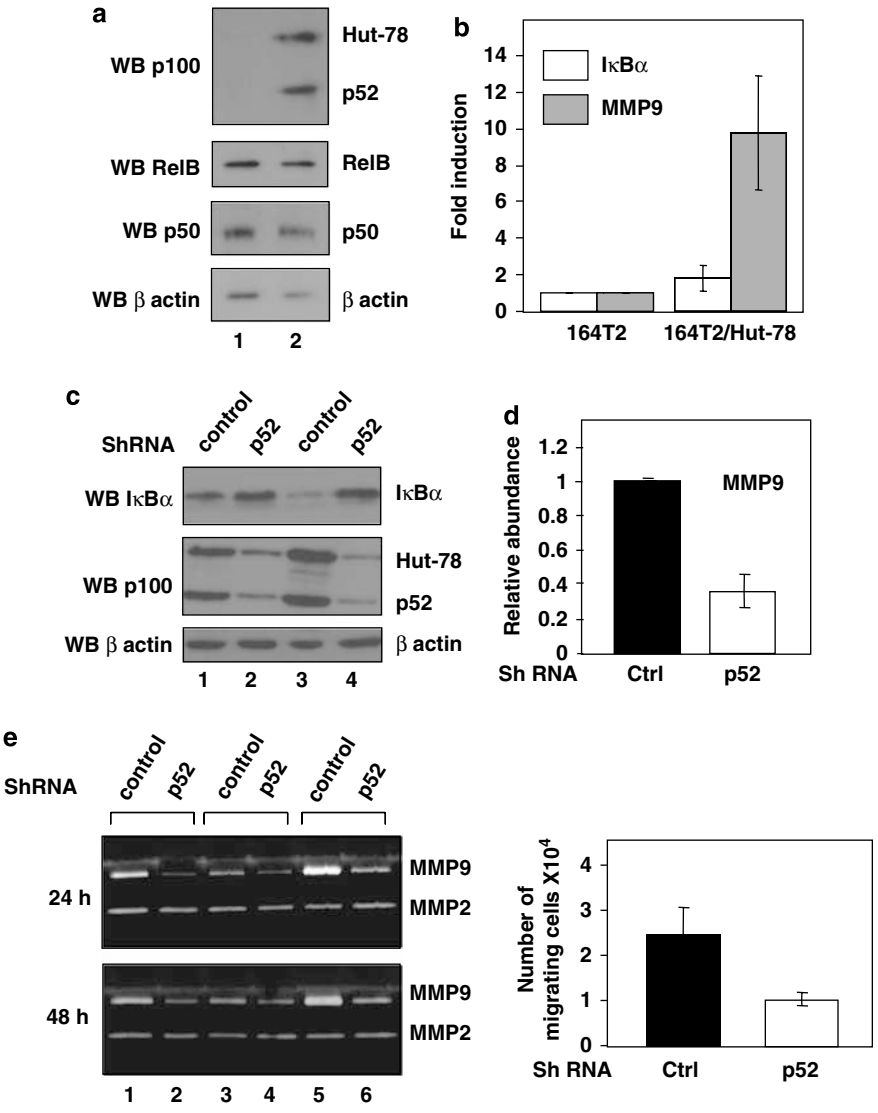

Figure 3 *MMP9* is a p52-dependent gene in lymphoma cells. (**a** and **b**) Hut-78 overexpression in a lymphoma cell line triggers *MMP9* but not *IκBα* gene expression. (**a**) Cell extracts from the 164T2 cell line stably transfected with an empty vector or with a FLAG-tagged Hut-78 expression plasmid (lanes 1 and 2, respectively) were subjected to western blot experiments using the anti-p100, anti-RelB, p50 or β-actin, as indicated. (**b**) Increased MMP9 but not IκBα mRNA levels on Hut-78 overexpression in 164T2 cells. MMP9 and IκBα mRNA levels using total RNAs from both Hut-78 expressing or control 164T2 cells were quantified by real-time PCR analysis. The figure shows the data from two independent experiments performed in duplicates and plotted as described above (mean values ± s.d.). (**c**) Establishment of p52-depleted HUT-78 cells. HUT-78 cells were infected with the indicated shRNA lentiviral construct and cell extracts from these infected cells were subjected to anti-IκBα, anti-p100 and β-actin western blot analysis. The figure shows the data obtained from two independent infections. (**d**) Decreased MMP9 mRNA levels on p52 depletion in HUT-78 cells. MMP9 mRNA levels using total RNAs from HUT-78 cells infected with the control or with the shRNA p52 lentiviral construct were quantified by real-time PCR analysis. MMP9 mRNA levels in HUT-78 cells infected with the control shRNA was set to 1 and levels of these transcripts in the other experimental condition were relative to that after normalization with 18S. The figure shows the data from five independent experiments performed in duplicates (mean values ± s.d.). (**e**) Impaired gelatinase activity and invasive potential in p52-depleted HUT-78 cells. On the left, conditional media from HUT-78 cells infected with the control shRNA or with the shRNA p52 for 24 or 48 h (top and bottom panels, respectively) were subjected to zymogram experiments using a SDS-polyacrylamide gel copolymerized with gelatine. The upper and lower bands correspond to MMP9 and MMP2 activities, respectively. On the right, HUT-78 infected with the indicated shRNA constructs were subjected to Matrigel invasion assays and the number of migrating cells was plotted. The Figure shows the representative results (mean values ± s.d.) from two independent infections.

expected, LTβ, but not TNFα, triggered p100 processing into p52 in these NEMO-deficient cells (Figure 4b, top panel, compare lane 1 with lanes 2–7), which confirmed that the NF-κB-alternative pathway is still functional in these cells. We observed that TNFα but not LTβ-mediated *MMP9* and *IκBα* inductions of gene expression were severely impaired in the NEMO-deficient MEFs (Figures 4c and d). Thus, our data suggest that *MMP9* gene expression is regulated by the alternative NF-κB-activating pathway in MEF cells.

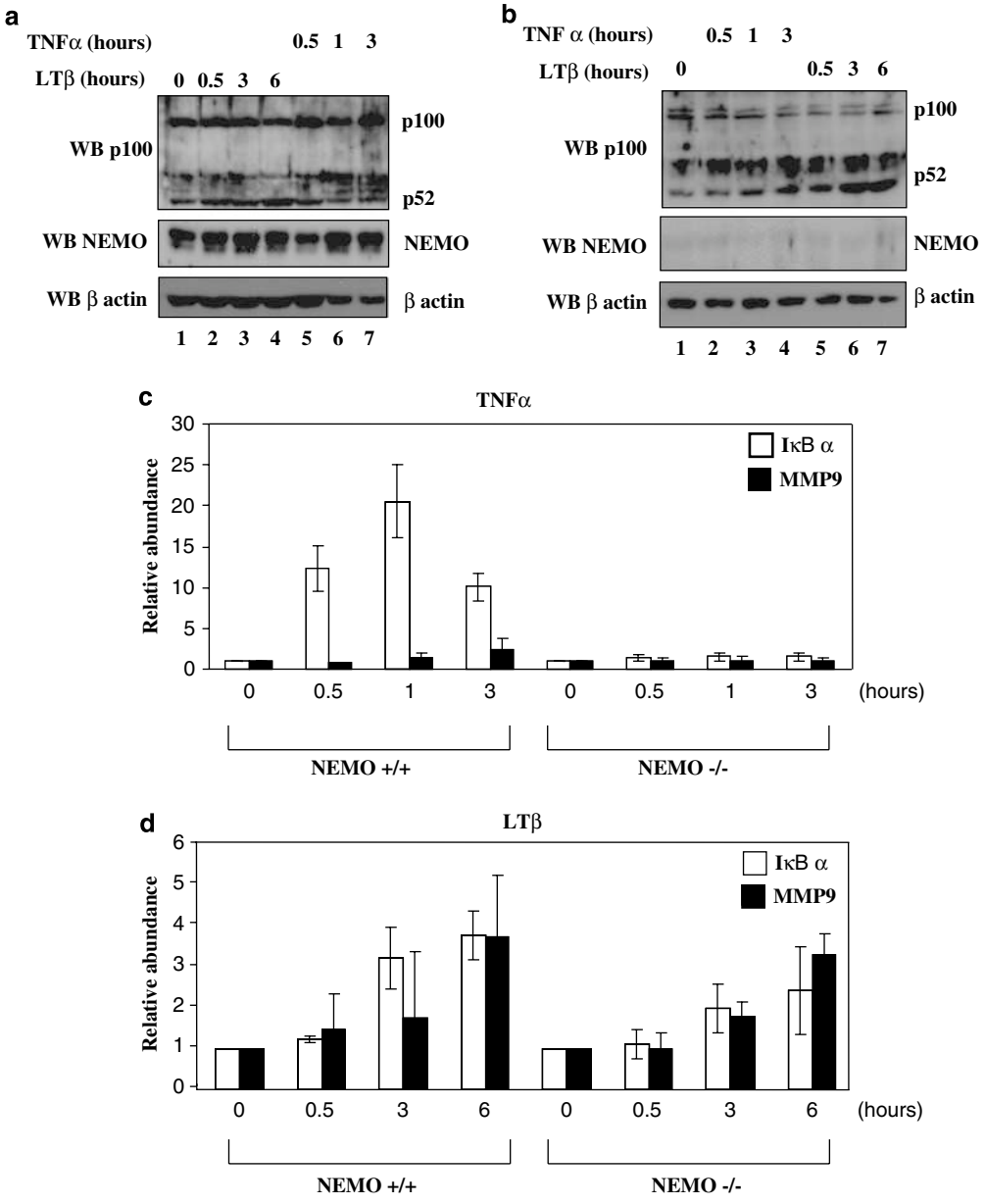

Figure 4 Induction of *MMP9* gene expression via the alternative nuclear factor (NF)-κB-activating signalling pathway. (**a**) p100 processing into p52 in lymphotoxin-β (LTβ)-stimulated but not tumor necrosis factor-α (TNFα)-stimulated wild-type mouse embryonic fibroblast (MEF) cells. MEF cells were left untreated (lane 1) or stimulated with the indicated periods of time with a LTβR agonistic antibody (lanes 2–4) or with TNFα (lanes 5–7) and cell extracts from those cells were subjected to anti-p100, anti-NEMO and anti-β-actin western blot analysis, as indicated. (**b**) Unaltered LTβ-mediated p100 processing into p52 in NEMO-deficient MEF cells. Same as in **a**. except that the treatments were performed on the NEMO-deficient MEF cells. (**c** and **d**) LTβ-mediated but not TNFα-mediated transcriptional induction of *MMP9* and *IκBα* in NEMO-deficient MEF cells. Total RNAs from TNFα-stimulated (**c**) or LTβ-stimulated (**d**) wild-type or NEMO-deficient cells were subjected to quantitative real-time PCR analysis to assess IκBα or MMP9 mRNA levels using the appropriate primers. The abundance of the IκBα or MMP9 mRNA levels in unstimulated cells was set to 1 and levels of both transcripts in TNFα or LTβ-stimulated cells were relative to that after normalization with glyceraldehyde-3-phosphate dehydrogenase (GAPDH). The figure shows the data from three independent experiments (mean values ± s.d.).

Hut-78 interacts with multiple NF-κB/IκB proteins, coactivators and corepressors

Transcriptional activators or coactivators should be part of these Hut-78 or p52-containing transcriptional complexes for the induction of *MMP9* gene expression. Immunofluorescence studies indicated that Hut-78 and p52 were nuclear whereas p100 was cytoplasmic (Figure 5b, top panels). A nuclear localization signal (NLS; RKRRK, amino acids 337–341) was identified within its Rel homology domain (RHD; Figure 5a; Neri *et al*., 1991). To prove the role of this sequence for the nuclear localization of Hut-78, we generated from one ('NLS 1' to 'NLS 5') to 4 amino-acid substitutions (NLS 1,2,3,4) within this NLS sequence and addressed the

localization of the resulting mutants by immunofluorescence. Although amino acids 337 and 341 were dispensable for the nuclear localization of Hut-78 as both the 'NLS1' and 'NLS5' mutants were mostly nuclear, amino acids 338 or 339 were essential as both 'NLS 2' and 'NLS 3' mutants were mostly cytoplasmic (Figure 5b). Such staining was even more dramatic with the 'NLS 1,2,3,4' mutant where amino acids 337–340 were substituted to alanine (Figure 5b). Mutation of this NLS did not prevent the constitutive processing into p52 (Figure 5c, compare lanes 2 and 3). Thus, the nuclear localization of Hut-78 requires the NLS sequence located within the RHD.

We next selected and tested several nuclear NF-κB proteins that harbour a transactivating domain for interaction with Hut-78. p65 and RelB bound this truncated NF-κB2 protein in HUT-78 cells (Figure 5d, top panel, lanes 3 and 4, respectively). Hut-78 was also found in the anti-p50 immunoprecipitate (Figure 5d, top panel, lane 2). Moreover, ectopically expressed FLAG-Hut-78 also bound overexpressed BCL-3, another oncogenic member of the IκB family that harbours two transactivation domains (Bours *et al*., 1993; Figure 5e, top panel, lane 3). Thus, Hut-78 interacts with multiple NF-κB proteins as well as HDAC proteins (see Supplementary Data section) in the nucleus.

p52 and Hut-78-mediated MMP9 transcriptional induction involves the recruitment of a H3K4 HMT complex

Covalent modifications of histones control chromatin structure and regulate gene expression (Shilatifard, 2006; Berger, 2007; Bhaumik *et al*., 2007). Histone

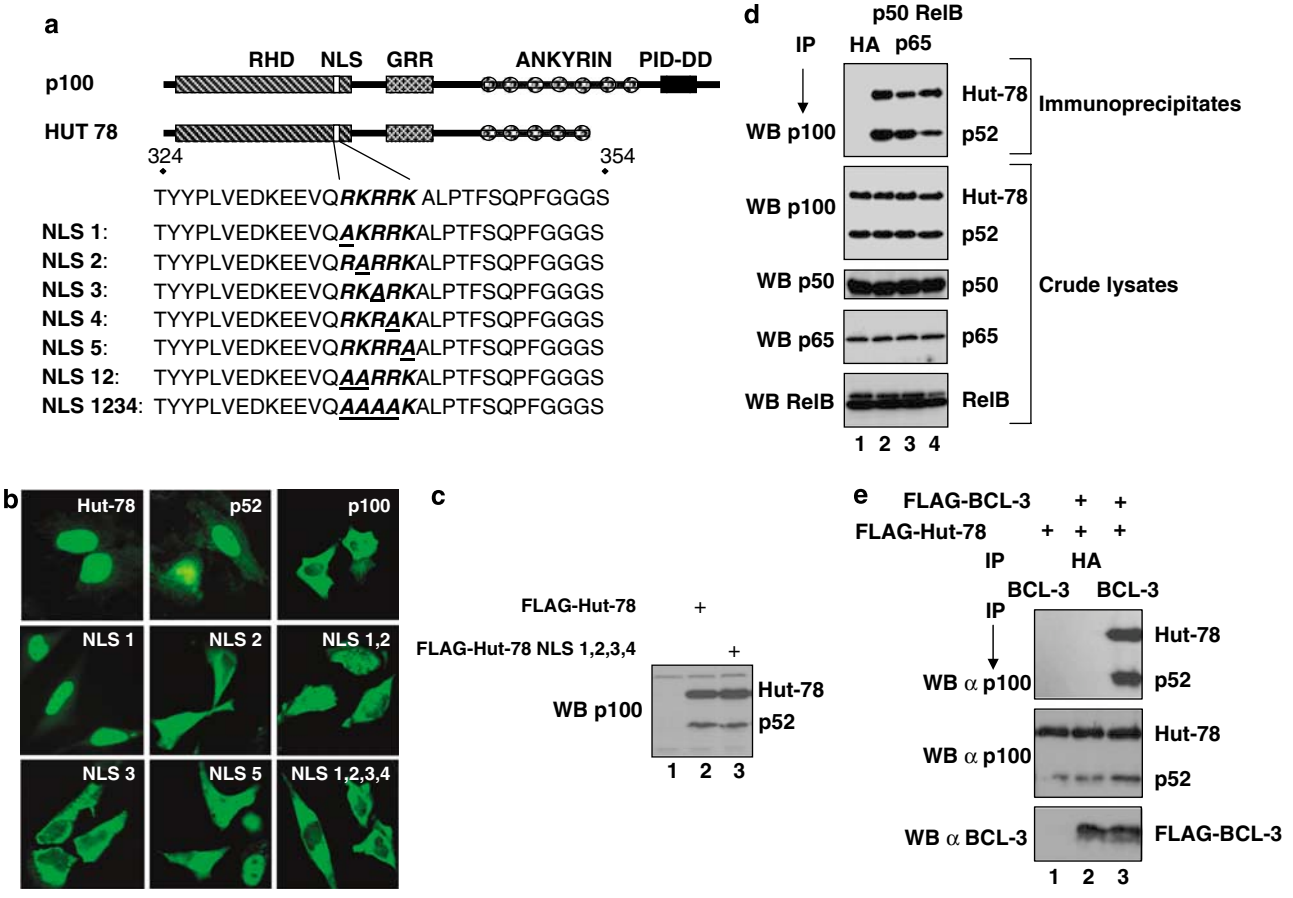

Figure 5 Hut-78 interacts with multiple nuclear factor (NF)-κB proteins and requires a functional NLS located within the RHD domain for its nuclear localization. (**a**) Schematic representation of wild-type NF-κB2/p100, Hut-78 and of Hut-78 mutants harbouring from 1 ('NLS 1' to 'NLS 5') to 4 lysine to alanine substitutions ('NLS 1234') within the nuclear localization sequence ('NLS'). RHD, Rel homology domain; PID, processing inhibitory domain; DD, death domain. (**b**) Hut-78 is a nuclear protein and harbours a functional NLS sequence. HeLa cells were transfected with 2 μg of the indicated expression vectors and analysed by immunofluorescence using an antiserum recognizing the N-terminal peptide of NF-κB2/p100 as primary antibody and fluorescein isothiocyanate (FITC)-conjugated anti-mouse IG as secondary antibody. (**c**) Constitutive processing of Hut-78, Hut-78 NLS 1234 and of the K75A mutant into p52. 293 cells were transfected with the indicated expression plasmids and an anti-p100 western blot was carried out on the cell extracts. (**d**) Hut-78 binds to multiple NF-κB proteins. Cell extracts from HUT-78 cells were subjected to anti-HA (negative control), -p50, -p65 or -RelB immunoprecipitations followed by anti-p100 western analysis (top panel, lanes 1–4, respectively). Cell extracts were also subjected to anti-p100, -p50, -p65 or -RelB analysis as well (bottom panels). (**e**) Hut-78 binds BCL-3. 293 cells were transfected with the indicated expression plasmids and anti-HA (negative control) or anti-BCL-3 immunoprecipitations followed by anti-p100 western analysis were carried out on the cell extracts, as indicated (top panel). Cell extracts were subjected to anti-p100 and anti-BCL-3 western analysis as well (bottom panels).

lysine methylation is involved in both gene activation and repression, depending on the identity of the lysine residue targeted for methylation. As di- and trimethylation at histone H3 lysine 4 are correlated with gene activation (Noma and Grewal, 2002; Santos-Rosa *et al*., 2002), we determined whether histone H3 was trimethylated at lysine 4 on the κB site of the *MMP9* promoter on p52 or Hut-78 overexpression by chromatin immunoprecipitation (ChIP) assays. A robust histone H3K4 trimethylation was detected on the *MMP9* but not on the *IκBα* promoter on p52 or Hut-78 overexpression in NIH3T3 cells (Figure 6b). This recruitment relies on p52 production as a much weaker H3K4 histone methyltransferase (HMT) activity was detected on the *MMP9* promoter in cells expressing the Hut-78 ΔGRR mutant (Figure 6b). Finally, the H3K4me3 activity on the *MMP9* promoter was impaired on p52 depletion in HUT-78 cells (Figure 6c). Thus, overexpressed p52 and Hut-78 induce *MMP9* expression by tethering a H3K4 HMT complex.

Whereas one multi-subunit complex (referred to as COMPASS and Set1 complex) that includes the *Drosophila* trithorax-related protein Set1 has been shown to trigger the mono-, di- and trimethylation of histone H3K4 in yeast (Briggs *et al*., 2001; Miller *et al*., 2001; Nagy *et al*., 2002; Noma and Grewal, 2002), multiple complexes harbouring robust H3K4 HMT activities have been isolated in mammalian cells and all of them contained one or two SET domain-containing homologues of yeast Set1 (Hughes *et al*., 2004; Glaser *et al*., 2006). As those distinct Set-1-like human H3K4 HMT complexes also share common subunits such as ASH2L, RBBP5 and WDR5, we determined whether those proteins interact with p52 by coimmunoprecipitation experiments. ASH2L bound p52, although not as strongly as BCL-3 did (used as a positive control; Figure 6d, top panel on the left, lanes 4 and 1, respectively). In contrast to ASH2L, both RBBP5 and WDR5 did not associate with p52 (Figure 6d, top panels on the middle and the right, compare lanes 2 with lanes 4). To explore whether Hut-78 is associated with some ASH2L-containing H3K4 HMTs at the endogenous level, we reasoned that those proteins presumably interacted in the chromatin. This was supported by the nuclear colocalization of Hut-78 but not of Hut-78 NLS 1234 with ASH2L (Figure 6e, panels on the right). We isolated the chromatin-associated proteins from HUT-78 cells, performed anti-ASH2L, -MLL1 and -MLL2 immunoprecipitations and noticed that Hut-78 bound ASH2L, MLL2 and to a less extent MLL1 (Figure 6f, lanes 2, 4 and 3, respectively). Thus, our data demonstrate that Hut-78 interacts with some H3K4 HMT complexes in the chromatin of HUT-78 cells.

To explore whether those H3K4 HMTs are recruited by p52 on the *MMP9* promoter, we investigated MLL1 and MLL2 (also named KMT2A and KMT2B, respectively; Allis *et al*., 2007) recruitments to this p52-regulated target gene by ChIP assays. Although we did not detect their recruitment on the *IκBα* promoter, both MLL1 and MLL2 proteins were tethered on the *MMP9* promoter in p52 overexpressing NIH3T3 cells (Figure 6g). Thus, our data suggest that p52 recruits the H3K4 HMT MLL1 and MLL2 complexes in a gene-specific manner.

Discussion

The *NF-κB2* translocation ultimately causes the loss of the inhibitory function of p100 and also p52 over-

Figure 6 Hut-78 and p52 recruit a H3K4 histone methyltransferase (HMT) on the κB site of the *MMP9* promoter. (**a**) Schematic representation of the promoter sequences of both *MMP9* and *IκBα* murine genes. The nuclear factor (NF)-κB, AP1/2, Sp1 binding sites and the TATA box are illustrated. The arrows indicate the primers used in chromatin immunoprecipitation (ChIP) assays. (**b**) Recruitment of a H3K4 HMT activity on the *MMP9* promoter via p52 and Hut-78. ChIP assays using an anti-H3K4me3 antibody were performed on DNA extracts from NIH3T3 cells infected with the empty pBabe, or the retrovirus expressing p52, Hut-78 or the Hut-78 ΔGRR mutant. Primers were derived from the promoter region of *MMP9* or *IκBα* genes and were designed to amplify a fragment that includes the κB sites. The recruitment of the H3K4me3 activity in the NIH3T3 cells infected with the empty pBabe construct was set to 1 and its levels in the other conditions were relative to that after normalization with H3. The figure shows the data from three independent experiments performed in duplicates (mean values ± s.d.). (**c**) Impaired recruitment of the H3K4me3 activity in p52-depleted HUT-78 cells. ChIP assays on HUT-78 cells infected with the indicated shRNA construct were carried out using an anti-H3K4me3 antibody. The signal obtained from a noncoding region (downstream of the albumin gene (Kouskouti and Talianidis, 2005)) was used to compensate for possible fluctuations arising during handling. The H3K4 me3 ChIP values in HUT-78 cells infected with the control shRNA construct was set to 1 and its value in the HUT-78 cells infected with the shRNA p52 was relative to that after normalization with the total H3 signal (as detected using the corresponding anti-H3 antibody). The figure shows the data obtained from five independent experiments performed on two distinct infections (means ± s.d.). (**d**) Association of p52 with ASH2L but not with RBBP5 and WDR5. 293 cells were transfected with the indicated expression plasmids and anti-FLAG immunoprecipitates followed by anti-p100 western blot analysis were carried out on the cell extracts (top panels). Anti-p100 and anti-FLAG western blots were performed on the crude cell extracts as well (bottom panels). (**e**) Hut-78 but not Hut-78 NLS 1234 colocalizes with ASH2L in the nucleus. HeLa cells were transfected with the indicated expression plasmids and anti-p100 or anti-HA immunofluorescences were carried out to detect Hut-78, Hut-78 NLS 1234 or ASH2L, respectively. (**f**) Association of Hut-78 with MLL1 and MLL2 in native chromatin-enriched extracts. Chromatin-associated proteins were isolated from highly purified and intact nuclei of HUT-78 cells (40×10^6 cells per experimental condition), as described (Aygun *et al*., 2008) and anti-HA (negative control), -ASH2L, -MLL1 and -MLL2 immunoprecipitates were carried out from those extracts, using the corresponding antibodies, followed by an anti-p100 western blot (panel on the left, lanes 1–4, respectively). Cell extracts were also subjected to anti-p100 western blot analysis (right panel). (**g**) Enhanced MLL1 and MLL2 recruitments to the *MMP9* but not the *IκBα* promoter on p52 overexpression in NIH3T3 cells. ChIP assays using an anti-MLL1 or anti-MLL2 antibody were performed on DNA extracts from NIH3T3 cells infected with the empty pBabe, or the retrovirus expressing p52. The recruitment of MLL1 or MLL2 in the NIH3T3 cells infected with the empty pBabe construct was set to 1 and its levels in the other conditions were relative to that after normalization with H3. The Figure shows the data from three (MLL1) or two (MLL2) independent experiments performed in duplicates (mean values ± s.d).

production. Although there is now experimental evidence for a key role of this chromosomal translocation in lymphomagenesis (Zhang *et al*., 2007), it remained unclear whether the loss of the inhibitory function of p100 and/or the overproduction of p52 is the underlying mechanism. There are several evidences for p52 being essential for the oncogenic potential of the truncated NF-κB2 proteins. First, p52 and a truncated p100

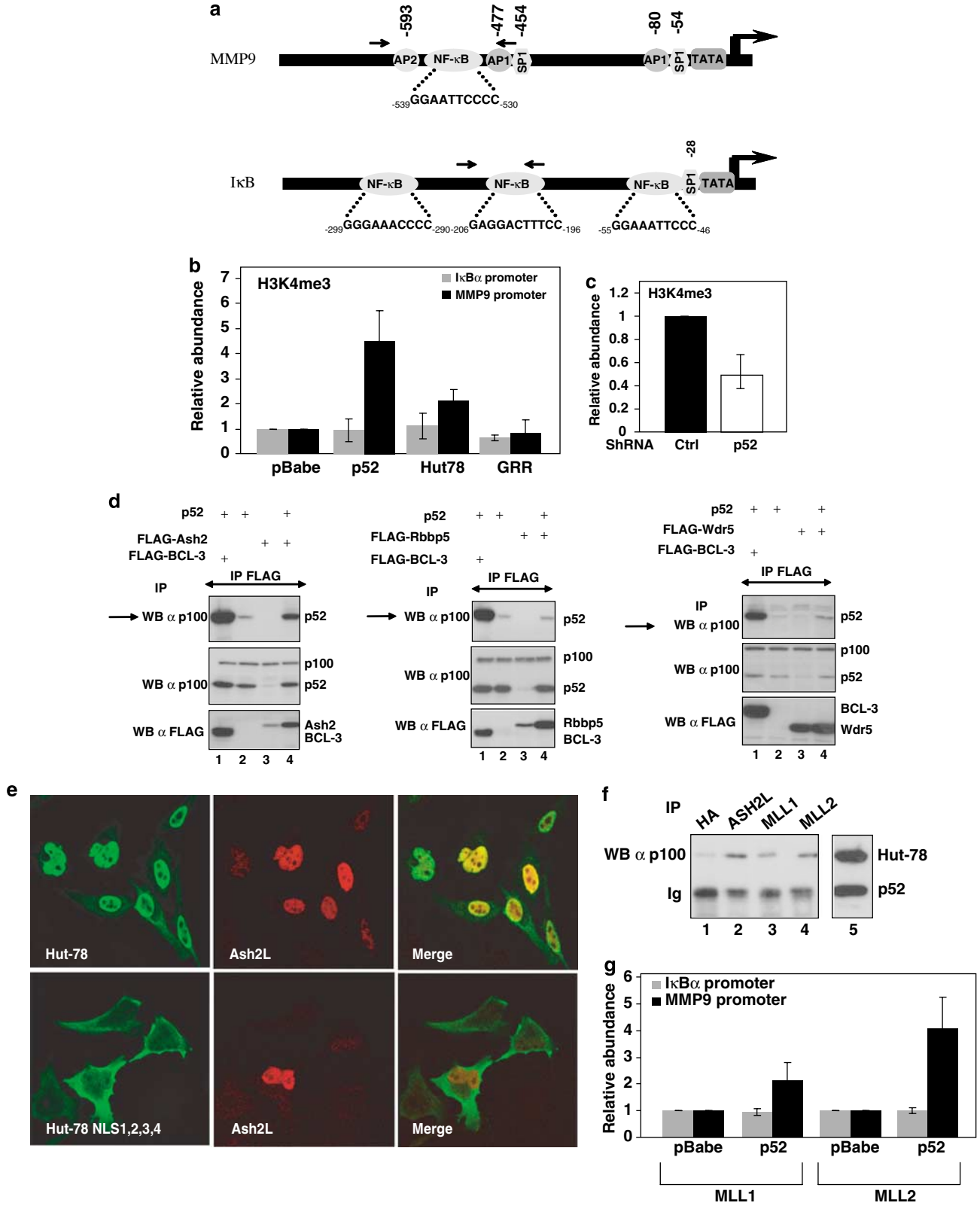

mutant that constitutively produces p52 are oncogenic *in vitro*, as judged by colony-formation assays performed in rat embryonic fibroblasts or in mouse FL5.12 cells (Qing *et al*., 2007). These data suggest that p52 overproduction is sufficient to trigger a transformation anchorage-independent growth in those cells and this was further supported by the very similar expression profile of many tumour-associated genes on overexpression of either p52 or the truncated p100 product (Qing *et al*., 2007). Our data support the notion that many tumour-associated genes are induced by the NF-κB2 truncated proteins via p52 production as MMP9 is similarly induced by p52 or Hut-78 but not by a mutant defective in processing. Nevertheless, other data challenged the notion that p52 overproduction alone drives lymphomagenesis. Indeed, constitutive production of p52 in lymphocytes is not tumorigenic in mice but rather predisposed to an inflammatory autoimmune disease through a sustained repression of Bim, a member of the antiapoptotic Bcl-2 family (Wang *et al*., 2008). In contrast to Hut-78, overexpressed p52 only transiently induced TRAF1 expression in lymphocytes and rather appeared to act as homodimers harbouring repressing transcriptional activities *in vitro* and *in vivo* (Wang *et al*., 2008). Those data are in agreement with earlier studies showing that Hut-78 harboured an enhanced transactivation potential compared to p52 (Chang *et al*., 1995; Epinat *et al*., 2000; Kim *et al*., 2000). Thus, overproduced p52 in lymphocytes triggers the expression of many common target genes, among which is *MMP9*, yet several genes such as *TRAF1* required to drive lymphomagenesis *in vivo* are specifically induced by Hut-78 but not by p52.

The enhanced *MMP9* expression seen on p52 overproduction highlights the fact that the constitutively activated alternative NF-κB pathway contributes to the pathogenesis of haematological disorders such as multiple myelomas and cutaneous T-cell lymphomas (Annunziata *et al*., 2007; Keats *et al*., 2007). In support for a role of this pathway in lymphomagenesis, NIK is overexpressed in some cases of T-cell leukaemias and in Hodgkin's lymphomas that do not express any oncogenic viral proteins (Saitoh *et al*., 2008). Levels of p52 are also increased in those NIK overexpressing haematological disorders and levels of MMP9 are decreased on NIK depletion through RNAi interference in these cells (Saitoh *et al*., 2008). Thus, these data, combined with our report, suggest that *MMP9* is a direct target gene of the NIK- and p100/p52-dependent signalling cascade.

Coactivators could be recruited by NF-κB/IκB proteins on selected promoters. Indeed, we demonstrated that overproduced p52 induces gene transcription by recruiting selected H3K4 HMT in a promoter-specific manner. Indeed, whereas p52 tethers MLL1 and MLL2 complexes on the *MMP9* gene promoter, it failed to do it on the *IκBα* promoter in NIH3T3 cells. This mechanism may explain why p52 significantly induces *MMP9* but not *IκBα* gene expression in these cells. Our data indeed suggest that the differential recruitment of H3K4 HMT complexes by NF-κB proteins will govern the ability of those target genes to be induced or not by those transcription factors. Several potential mechanisms underlying the recruitment of H3K4 HMT complexes to the target genes were discussed (Ruthenburg *et al*., 2007). One hypothesis is the direct recruitment of H3K4 HMT complexes to selected promoters by the DNA binding factors whereas the MLL core complex components (WDR5, RBBP5 and ASH2L) would regulate the activity but not the recruitment of those enzymatic complexes to their target loci. Our data favour this hypothesis as we show here that a Hut-78 mutant that does not generate p52 did not efficiently drive *MMP9* gene expression, at least in part because it failed to properly recruit an H3K4me3 enzymatic activity on the promoter of this gene. Our data highlight a promoter-specific recruitment of selected H3K4 HMT complexes by an oncogenic NF-κB/IκB protein, yet the molecular mechanisms underlying this gene-specific effect remains totally unknown. It will be of great interest to experimentally address to which extent the post-translational modifications of the NF-κB/IκB proteins themselves in response to various signals ultimately regulate the ability of those transcription factors to recruit H3K4 HMT complexes on the promoters of their target genes.

H3K4 me3 is a dynamic modification (Berger, 2007) and a family of proteins sharing the Jumonji C (JmjC) domain were showed to catalyse site-specific demethylation of mono-, di- and trimethylated histones (Klose *et al*., 2006). Among them is RBP2, a demethylase that specifically catalyses demethylation on H3K4 (Klose *et al*., 2007). Whether this demethylase regulates the expression of the NF-κB target genes remains an open question but our data strongly suggest that the recruitment of NF-κB proteins that positively regulate gene transcription may involve the concomitant removal of H3K4 demethylases from the promoter of those NF-κB-dependent genes. Importantly, the H3K27 demethylase Jmjd3 whose inducible expression in lipopolysaccharide-stimulated macrophages is NF-κB dependent was found associated with WDR5 and RBBP5, the core subunits of the H3K4 HMT MLL complexes, a result that support the existence of a functional cross-talk between changes in H3K4me3 and H3K27me3 (De Santa *et al*., 2007). This study, combined with our report, opens unexplored avenues of research whose goal will be to define the contribution of those lysine-specific demethylases in the regulation of NF-κB target genes in health and in diseases.

Materials and methods

Cell culture, biological reagents and treatments

Human embryonic kidney 293, HeLa and NIH3T3 cells as well as wild-type or NEMO-deficient immortalized mouse embryonic fibroblasts, a gift from Dr M Pasparakis (Institute for Genetics, Centre for Molecular Medicine (CMMC), University of Cologne, Germany), were maintained in Dulbecco's modified Eagle's medium supplemented with 10% fetal calf serum (FCS; Life Technologies, Grand Island, NY, USA), glutamine and antibiotics. HUT-78 cells were cultured in

RPMI medium supplemented with 10% FCS, glutamine and antibiotics. The lymphoma cell line 164T2, a gift from Dr Y St-Pierre (INRS-Institut Armand-Frappier, University of Québec, Laval, Québec, Canada), was cultured as described (Aoudjit *et al*., 1998). TNFα was from Roche Applied Sciences (Indianapolis, IN, USA) whereas the generation of the LTβR agonistic antibody was previously described (Dejardin *et al*., 2002).

Details on expression constructs and antiserum sources are described in Supplementary Data.

Immunoprecipitations, immunofluorescences and isolation of enriched native chromatin extracts

Immunoprecipitations in 293 cells were carried out as previously described (Viatour *et al*., 2003). For immunofluorescence studies, HeLa cells were seeded in six-well plates and subsequently transfected with the indicated expression plasmids using FUGENE 6 (Roche). Twenty-four hours later, cells were washed with phosphate-buffered saline, fixed with 4% paraformaldehyde and permeabilized with ethanol for 6 min at −20 °C. Fixed cells were incubated with monoclonal anti-p100 antibodies for 45 min at 37°C followed by a 45 min incubation at RT with fluorescein isothiocyanate-conjugated anti-mouse immunoglobulin G (Dako, Glostrup, Denmark). Coverslips were then mounted with Prolong Gold Antifade (Invitrogen, Carlsbad, CA, USA) and cells were observed by fluorescent microscopy (Nikon).

Preparation of enriched native chromatin extracts from HUT-78 cells were carried out as described (Aygun *et al*., 2008).

Retroviral and lentiviral infections of NIH3T3 and HUT-78 cells

Retroviral infections of NIH3T3 cells were performed as described (Viatour *et al*., 2004). For lentiviral infections of HUT-78 cells, 293FT cells were transfected with 12 μg of the 'non-target' lentiviral shRNA plasmid (used as negative control) or the shRNA construct that targets p100/p52 (NM_002502.2) with the following sequence 5′-CCGG CCCTATCACAAGATGAAGATTCTCGAGAATCTTCAT CTTGTGATAGGGTTTTT-3′ and with 12 and 5 μg of R8.91 and VSVG plasmids, respectively. The supernatants from those infected cells were collected 48 h after transfection, added with polybrene to 5×10^5 HUT-78 cells and subjected to centrifugation for 10 min at 1200 r.p.m. This later step was repeated the next day and HUT-78 cells were treated with puromycine (1 μg/ml) 48 h after the last infection.

Zymograms

Conditioned media of cells incubated in serum-free RPMI for 24 or 48 h were collected and centrifuged. Supernatant (18 μl) mixed with 6 μl of loading buffer were applied onto a 10% polyacrylamide gel copolymerized with gelatin (1 mg/ml). After electrophoresis, gels were renatured in 2% Triton X-100 for 1 h and incubated overnight at 37 °C in a buffer consisting of 50 mM Tris-HCl (pH7.6) and 10 mM $CaCl_2$. The gels were then stained with Coomassie brilliant blue in 40% methanol and 10% acetic acid and destained in 20% methanol and 10% acetic acid. Gelatinase activities were detected as transparent bands on the blue background.

Matrigel invasion assay

The assay was performed using a 24-well polycarbonate transwell permeable support with 8 μm pores (Corning Costar), coated with 6.21 μg of Matrigel (BD Biosciences, Bedford, MA, USA). HUT-78 cells infected with distinct shRNA constructs were suspended in serum-free RPMI at a concentration of 5.10^5 cells/ml and 100 μl were loaded into top chambers. The lower chambers were filled with 0.6 ml RPMI containing 10% fetal bovine serum. After 72 h of incubation at 37 °C in a humidified 5% CO_2 incubator, cells that migrated through the Matrigel-coated filters were recovered from the lower compartment and counted using a Thoma hemocytometer.

Affymetrix microarray analysis

Total RNAs were extracted from NIH3T3 cells stably infected with empty virus or virus expressing p52 or Hut-78 and cultured in triplicates, using the RNeasy Minit kit from Qiagen (Valencia, CA, USA). The integrity of the RNAs from those nine distinct experimental conditions was checked with the Agilent Bioanalyzer using the RNA 6000 Nano kit (Agilent, Santa Clara, CA, USA). Biotin-labelled cRNA and subsequent hybridization and scanning were performed following the manufacturer's instructions.

Real-Time PCRs and ChIP assays

Total RNAs were extracted using the EZNA Total RNA kit (Omega Bio-tek, Norcross, GA, USA) and cDNAs were synthesized using the RevertAid H Minus First Strand cDNA Synthesis kit (Fermentas, Glen Burnie, MD, USA). Subsequent PCRs were carried out using the Power SYBR Green PCR master kit (Applied Biosystems, Foster City, CA, USA) on the LightCycler 480 (Roche). Primers to amplify IκBα and MMP9 sequences from NIH3T3 and HUT-78 cells as well as for the amplification of glyceraldehyde-3-phosphate dehydrogenase and 18S sequences (for normalization purposes in NIH3T3 and HUT-78 cells, respectively) are available on request.

For ChIP assays, cells were cross-linked with 1% paraformaldehyde and sonicated using the Bioruptor (Diagenode). ChIP assays were performed using the OneDay ChIP kit (Diagenode) using $1.5–2 \times 10^6$ cells per experimental condition. Subsequent PCRs were carried out using the Power SYBR Green PCR master kit (Applied Biosystems) on the LightCycler 480 (Roche). Input DNA was analysed simultaneously and used as normalization. For normalization of the ChIP assays in HUT-78 cells, the signal obtained from a non-coding region (downstream of the albumin gene (Kouskouti and Talianidis, 2005) was used to compensate for possible fluctuations arising during handling. For the histone-related ChIPs, H3K4me3 ChIP values were normalized according to the total H3 signal (as detected using the corresponding anti-H3 antibody).

Acknowledgements

We are grateful to F Fuks for helpful discussions, to M Pasparakis, Y St-Pierre and R Weil for the gifts of wild-type and NEMO-deficient mouse embryonic fibroblasts, the 164T2 cell line and the anti-NEMO antibody, respectively. We also thank Dr J-H Lee, Dr DG Skalnik and Dr C van Lint for the gift of expression plasmids. M-PM, LdeL and AC are Senior Research Associates whereas ED is Research Associate at the Belgian National fund for Research ('FNRS'). IR and XZ are 'TELEVIE' Research Assistants whereas MA and AK are 'FNRS' Research Assistants. This work was supported by grants from the University of Liege (ULg), FNRS, TELEVIE, the Belgian Federation against Cancer, the IAP6/18 (funded by the Interuniversity Attraction Poles Programme, initiated by the Belgian State, Science Policy Office), the 'Centre Anti-Cancéreux' and 'Fonds Léon Frédéricq' (Faculty of Medicine, ULg).

References

Allis CD, Berger SL, Cote J, Dent S, Jenuwien T, Kouzarides T *et al*. (2007). New nomenclature for chromatin-modifying enzymes. *Cell* **131**: 633–636.

Annunziata CM, Davis RE, Demchenko Y, Bellamy W, Gabrea A, Zhan F *et al*. (2007). Frequent engagement of the classical and alternative NF-kappaB pathways by diverse genetic abnormalities in multiple myeloma. *Cancer Cell* **12**: 115–130.

Aoudjit F, Potworowski EF, St-Pierre Y. (1998). The metastatic characteristics of murine lymphoma cell lines *in vivo* are manifested after target organ invasion. *Blood* **91**: 623–629.

Aygun O, Svejstrup J, Liu Y. (2008). A RECQ5-RNA polymerase II association identified by targeted proteomic analysis of human chromatin. *Proc Natl Acad Sci USA* **105**: 8580–8584.

Berger SL. (2007). The complex language of chromatin regulation during transcription. *Nature* **447**: 407–412.

Bhaumik SR, Smith E, Shilatifard A. (2007). Covalent modifications of histones during development and disease pathogenesis. *Nat Struct Mol Biol* **14**: 1008–1016.

Bonizzi G, Karin M. (2004). The two NF-kappaB activation pathways and their role in innate and adaptive immunity. *Trends Immunol* **25**: 280–288.

Bours V, Franzoso G, Azarenko V, Park S, Kanno T, Brown K *et al*. (1993). The oncoprotein Bcl-3 directly transactivates through kappa B motifs via association with DNA-binding p50B homodimers. *Cell* **72**: 729–739.

Briggs SD, Bryk M, Strahl BD, Cheung WL, Davie JK, Dent SY *et al*. (2001). Histone H3 lysine 4 methylation is mediated by Set1 and required for cell growth and rDNA silencing in Saccharomyces cerevisiae. *Genes Dev* **15**: 3286–3295.

Cabannes E, Khan G, Aillet F, Jarrett RF, Hay RT. (1999). Mutations in the IkBa gene in Hodgkin's disease suggest a tumour suppressor role for IkappaBalpha. *Oncogene* **18**: 3063–3070.

Chang CC, Zhang J, Lombardi L, Neri A, Dalla-Favera R. (1995). Rearranged NFKB-2 genes in lymphoid neoplasms code for constitutively active nuclear transactivators. *Mol Cell Biol* **15**: 5180–5187.

Claudio E, Brown K, Park S, Wang H, Siebenlist U. (2002). BAFF-induced NEMO-independent processing of NF-kappa B2 in maturing B cells. *Nat Immunol* **3**: 958–965.

Coope HJ, Atkinson PG, Huhse B, Belich M, Janzen J, Holman MJ *et al*. (2002). CD40 regulates the processing of NF-kappaB2 p100 to p52. *EMBO J* **21**: 5375–5385.

Courtois G, Gilmore TD. (2006). Mutations in the NF-kappaB signaling pathway: implications for human disease. *Oncogene* **25**: 6831–6843.

De Santa F, Totaro MG, Prosperini E, Notarbartolo S, Testa G, Natoli G. (2007). The histone H3 lysine-27 demethylase Jmjd3 links inflammation to inhibition of polycomb-mediated gene silencing. *Cell* **130**: 1083–1094.

Dejardin E, Droin NM, Delhase M, Haas E, Cao Y, Makris C *et al*. (2002). The lymphotoxin-beta receptor induces different patterns of gene expression via two NF-kappaB pathways. *Immunity* **17**: 525–535.

Derudder E, Laferte A, Ferreira V, Mishal Z, Baud V, Tarantino N *et al*. (2003). Identification and characterization of p100HB, a new mutant form of p100/NF-kappa B2. *Biochem Biophys Res Commun* **308**: 744–749.

Emmerich F, Meiser M, Hummel M, Demel G, Foss HD, Jundt F *et al*. (1999). Overexpression of I kappa B alpha without inhibition of NF-kappaB activity and mutations in the I kappa B alpha gene in Reed-Sternberg cells. *Blood* **94**: 3129–3134.

Epinat JC, Kazandjian D, Harkness DD, Petros S, Dave J, White DW *et al*. (2000). Mutant envelope residues confer a transactivation function onto N-terminal sequences of the v-Rel oncoprotein. *Oncogene* **19**: 599–607.

Fracchiolla NS, Lombardi L, Salina M, Migliazza A, Baldini L, Berti E *et al*. (1993). Structural alterations of the NF-kappa B transcription factor lyt-10 in lymphoid malignancies. *Oncogene* **8**: 2839–2845.

Glaser S, Schaft J, Lubitz S, Vintersten K, van der Hoeven F, Tufteland KR *et al*. (2006). Multiple epigenetic maintenance factors implicated by the loss of Mll2 in mouse development. *Development* **133**: 1423–1432.

Hayden MS, Ghosh S. (2008). Shared principles in NF-kappaB signaling. *Cell* **132**: 344–362.

Heissig B, Hattori K, Friedrich M, Rafii S, Werb Z. (2003). Angiogenesis: vascular remodeling of the extracellular matrix involves metalloproteinases. *Curr Opin Hematol* **10**: 136–141.

Hughes CM, Rozenblatt-Rosen O, Milne TA, Copeland TD, Levine SS, Lee JC *et al*. (2004). Menin associates with a trithorax family histone methyltransferase complex and with the hoxc8 locus. *Mol Cell* **13**: 587–597.

Ishikawa H, Carrasco D, Claudio E, Ryseck RP, Bravo R. (1997). Gastric hyperplasia and increased proliferative responses of lymphocytes in mice lacking the COOH-terminal ankyrin domain of NF-kappaB2. *J Exp Med* **186**: 999–1014.

Jost PJ, Ruland J. (2007). Aberrant NF-kappaB signaling in lymphoma: mechanisms, consequences, and therapeutic implications. *Blood* **109**: 2700–2707.

Jungnickel B, Staratschek-Jox A, Brauninger A, Spieker T, Wolf J, Diehl V *et al*. (2000). Clonal deleterious mutations in the IkappaBalpha gene in the malignant cells in Hodgkin's lymphoma. *J Exp Med* **191**: 395–402.

Karin M, Lin A. (2002). NF-kappaB at the crossroads of life and death. *Nat Immunol* **3**: 221–227.

Keats JJ, Fonseca R, Chesi M, Schop R, Baker A, Chng WJ *et al*. (2007). Promiscuous mutations activate the noncanonical NF-kappaB pathway in multiple myeloma. *Cancer Cell* **12**: 131–144.

Keutgens A, Robert I, Viatour P, Chariot A. (2006). Deregulated NF-kappaB activity in haematological malignancies. *Biochem Pharmacol* **72**: 1069–1080.

Kim KE, Gu C, Thakur S, Vieira E, Lin JC, Rabson AB. (2000). Transcriptional regulatory effects of lymphoma-associated NFKB2/lyt10 protooncogenes. *Oncogene* **19**: 1334–1345.

Klose RJ, Kallin EM, Zhang Y. (2006). JmjC-domain-containing proteins and histone demethylation. *Nat Rev Genet* **7**: 715–727.

Klose RJ, Yan Q, Tothova Z, Yamane K, Erdjument-Bromage H, Tempst P *et al*. (2007). The retinoblastoma binding protein RBP2 is an H3K4 demethylase. *Cell* **128**: 889–900.

Kouskouti A, Talianidis I. (2005). Histone modifications defining active genes persist after transcriptional and mitotic inactivation. *EMBO J* **24**: 347–357.

Lalancette M, Aoudjit F, Potworowski EF, St-Pierre Y. (2000). Resistance of ICAM-1-deficient mice to metastasis overcome by increased aggressiveness of lymphoma cells. *Blood* **95**: 314–319.

Li Q, Verma IM. (2002). NF-kappaB regulation in the immune system. *Nat Rev Immunol* **2**: 725–734.

McKeithan TW, Rowley JD, Shows TB, Diaz MO. (1987). Cloning of the chromosome translocation breakpoint junction of the t(14;19) in chronic lymphocytic leukemia. *Proc Natl Acad Sci USA* **84**: 9257–9260.

Miller T, Krogan NJ, Dover J, Erdjument-Bromage H, Tempst P, Johnston M *et al*. (2001). COMPASS: a complex of proteins associated with a trithorax-related SET domain protein. *Proc Natl Acad Sci USA* **98**: 12902–12907.

Mori N, Sato H, Hayashibara T, Senba M, Hayashi T, Yamada Y *et al*. (2002). Human T-cell leukemia virus type I Tax transactivates the matrix metalloproteinase-9 gene: potential role in mediating adult T-cell leukemia invasiveness. *Blood* **99**: 1341–1349.

Nagy PL, Griesenbeck J, Kornberg RD, Cleary ML. (2002). A trithorax-group complex purified from Saccharomyces cerevisiae is required for methylation of histone H3. *Proc Natl Acad Sci USA* **99**: 90–94.

Neri A, Chang CC, Lombardi L, Salina M, Corradini P, Maiolo AT *et al*. (1991). B cell lymphoma-associated chromosomal translocation involves candidate oncogene lyt-10, homologous to NF-kappa B p50. *Cell* **67**: 1075–1087.

Noma K, Grewal SI. (2002). Histone H3 lysine 4 methylation is mediated by Set1 and promotes maintenance of active chromatin states in fission yeast. *Proc Natl Acad Sci USA* **99**(Suppl 4): 16438–16445.

Perkins ND. (2007). Integrating cell-signalling pathways with NF-kappaB and IKK function. *Nat Rev Mol Cell Biol* **8**: 49–62.

Qing G, Qu Z, Xiao G. (2007). Endoproteolytic processing of C-terminally truncated NF-kappaB2 precursors at kappaB-containing promoters. *Proc Natl Acad Sci USA* **104**: 5324–5329.

Redondo-Munoz J, Escobar-Diaz E, Samaniego R, Terol MJ, Garcia-Marco JA, Garcia-Pardo A. (2006). MMP-9 in B-cell chronic lymphocytic leukemia is up-regulated by alpha4beta1 integrin or CXCR4 engagement via distinct signaling pathways, localizes to podosomes, and is involved in cell invasion and migration. *Blood* **108**: 3143–3151.

Ruthenburg AJ, Allis CD, Wysocka J. (2007). Methylation of lysine 4 on histone H3: intricacy of writing and reading a single epigenetic mark. *Mol Cell* **25**: 15–30.

Saitoh Y, Yamamoto N, Dewan MZ, Sugimoto H, Martinez Bruyn VJ, Iwasaki Y *et al*. (2008). Overexpressed NF-kappaB-inducing kinase contributes to the tumorigenesis of adult T-cell leukemia and Hodgkin Reed-Sternberg cells. *Blood* **111**: 5118–5129.

Sakata K, Satoh M, Someya M, Asanuma H, Nagakura H, Oouchi A *et al*. (2004). Expression of matrix metalloproteinase 9 is a prognostic factor in patients with non-Hodgkin lymphoma. *Cancer* **100**: 356–365.

Santos-Rosa H, Schneider R, Bannister AJ, Sherriff J, Bernstein BE, Emre NC *et al*. (2002). Active genes are tri-methylated at K4 of histone H3. *Nature* **419**: 407–411.

Shilatifard A. (2006). Chromatin modifications by methylation and ubiquitination: implications in the regulation of gene expression. *Annu Rev Biochem* **75**: 243–269.

Shim JH, Xiao C, Paschal AE, Bailey ST, Rao P, Hayden MS *et al*. (2005). TAK1, but not TAB1 or TAB2, plays an essential role in multiple signaling pathways *in vivo*. *Genes Dev* **19**: 2668–2681.

Siebenlist U, Brown K, Claudio E. (2005). Control of lymphocyte development by nuclear factor-kappaB. *Nat Rev Immunol* **5**: 435–445.

Srivastava AK, Qin X, Wedhas N, Arnush M, Linkhart TA, Chadwick RB *et al*. (2007). Tumor necrosis factor-alpha augments matrix metalloproteinase-9 production in skeletal muscle cells through the activation of transforming growth factor-beta-activated kinase 1 (TAK1)-dependent signaling pathway. *J Biol Chem* **282**: 35113–35124.

Thakur S, Lin HC, Tseng WT, Kumar S, Bravo R, Foss F *et al*. (1994). Rearrangement and altered expression of the NFKB-2 gene in human cutaneous T-lymphoma cells. *Oncogene* **9**: 2335–2344.

Viatour P, Dejardin E, Warnier M, Lair F, Claudio E, Bureau F *et al*. (2004). GSK3-mediated BCL-3 phosphorylation modulates its degradation and its oncogenicity. *Mol Cell* **16**: 35–45.

Viatour P, Legrand-Poels S, van Lint C, Warnier M, Merville MP, Gielen J *et al*. (2003). Cytoplasmic IkappaBalpha increases NF-kappaB-independent transcription through binding to histone deacetylase (HDAC) 1 and HDAC3. *J Biol Chem* **278**: 46541–46548.

Wang Z, Zhang B, Yang L, Ding J, Ding HF. (2008). Constitutive production of NF-kappaB2 p52 is not tumorigenic but predisposes mice to inflammatory autoimmune disease by repressing Bim expression. *J Biol Chem* **283**: 10698–10706.

Xiao G, Harhaj EW, Sun SC. (2001). NF-kappaB-inducing kinase regulates the processing of NF-kappaB2 p100. *Mol Cell* **7**: 401–409.

Yoshizaki T, Sato H, Furukawa M, Pagano JS. (1998). The expression of matrix metalloproteinase 9 is enhanced by Epstein-Barr virus latent membrane protein 1. *Proc Natl Acad Sci USA* **95**: 3621–3626.

Zhang B, Wang Z, Li T, Tsitsikov EN, Ding HF. (2007). NF-kappaB2 mutation targets TRAF1 to induce lymphomagenesis. *Blood* **110**: 743–751.

Zhang J, Chang CC, Lombardi L, Dalla-Favera R. (1994). Rearranged NFKB2 gene in the HUT78 T-lymphoma cell line codes for a constitutively nuclear factor lacking transcriptional repressor functions. *Oncogene* **9**: 1931–1937.

Supplementary Information accompanies the paper on the Oncogene website (http://www.nature.com/onc)